Role of Sugarcane Bagasse Ash in Developing Sustainable Engineered Cementitious Composites

Muhammad Nasir Amin[1]*, Muhammad Ashraf[2], Rabinder Kumar[2], Kaffayatullah Khan[1], Daniyal Saqib[3], Syed Sajid Ali[3] and Sajidullah Khan[3]

[1] Department of Civil and Environmental Engineering, College of Engineering, King Faisal University, Al-Ahsa, Saudi Arabia,
[2] Department of Civil Engineering, Ghulam Ishaq Khan Institute of Engineering Sciences and Technology, Topi, Pakistan,
[3] Department of Civil Engineering, COMSATS University Islamabad, Abbottabad Campus, Islamabad, Pakistan

Sugarcane bagasse is an agricultural waste that can be transformed by incineration into a cement replacement material for various cementing purposes. This study investigated the role of finely ground bagasse ash (GBA) in producing engineered cementitious composites (ECCs) with the addition of polyvinyl alcohol (PVA) fibers. The main focus of this study was to develop a green ECC with higher strength capabilities (compressive, tensile, and flexural) and greater tensile ductility. To develop this composite, GBA was added into ECC mixes at different proportions, i.e., 10, 20, and 30%. The proportions of PVA fibers and the water-to-binder ratio were kept constant. The results revealed that the ECC mix containing 10% GBA exhibited higher compressive strength compared to that of a control and the other ECC mixes. The tensile and flexural strengths of the ECCs exhibited patterns almost similar to that of compressive strength. Moreover, the deflection in the control mix was higher compared to that of the GBA-ECC mixes at an initial curing age. The ECC mix containing 10% GBA exhibited better ductile behavior among all the ECC mixes used in this study.

Keywords: bagasse ash, engineered cementitious composite, compressive strength, tensile strength, flexural strength, ductility

INTRODUCTION

After water, concrete is the most widely used material on our planet. The estimated yearly consumption of concrete is approaching 30 billion tons (Klee, 2009). For the last two decades, the trend of using high-strength concrete has been increasing due to its demand for building advanced infrastructures. However, with the increase in strength, the brittleness of concrete also increases, which ultimately leads to the cracking and failure of concrete structures. Thus, it was decided to develop new cementitious materials with high ductility that would be more valuable in terms of safety, durability, and sustainability in structural applications. Therefore, a new composite material called engineered cementitious composite (ECC) was developed, which possessed high tensile strength along with high compressive strength (Li, 1993, 2002; Li et al., 2002). In ECC, the concrete is sustained on an increased loading rate even after first cracking while undergoing large deformation. Because of these properties, ECCs are also known as strain-hardening cementitious composites. In fact, the failure in concrete is initiated due to the generation of microcracks followed by their transformation into macrocracks. However, the addition of dispersed fibers into the matrix

has been observed to enhance the tensile properties of concrete and prevent microcracking from propagating to the macrocracking stage, which eventually prevents brittle failure (Al Qadi and Al-Zaidyeen, 2014). Apart from their well-known extreme tensile ductility (Li, 2012), ECCs have been engineered to demonstrate other useful traits, including light weight, low carbon footprint, self-healing, self-sensing, self-thermal control, impact resistance, fire resistance with low thermal conductivity, rapid setting, self-consolidation, spray-ability, and extrudability (Wu et al., 2012; Liu and Tan, 2018; Shi et al., 2018). However, all the above-mentioned traits greatly vary depending on the proportions, material type, and mix design of ECC.

The cement content in ECCs compared to that in normal concrete is quite high as it does not contain coarse aggregates. However, the increased cement contents not only creates more heat of hydration, autogenous shrinkage and higher costs, but also causes the emission of large amounts of CO_2 into the environment from the calcination of limestone and fuel combustion during the manufacturing of cement clinker (Zeman, 2009). Approximately, one ton of cement releases one ton CO_2, which is responsible for 5% of greenhouse gas emissions (Kumar et al., 2017). To minimize greenhouse effects, the addition of industrial byproducts and agricultural wastes have been observed as sustainable alternatives because they successfully replace bulk proportions of cement in ECCs without compromising strength and ductility (Kumar et al., 2017; Shafiq et al., 2018).

Currently, there is an increasing use of industrial waste, including fly ash, silica fume, and ground granulated blast furnace slag to produce highly sustainable concretes. The amorphous mineralogical character and high silicon dioxide (SiO_2) content of these materials are usually responsible for controlling the stability and the development of high strength in the end product (Shafiq et al., 2018). In addition, the trend of using biowastes from fuel sources in concrete, such as wheat straw ash, palm oil fuel ash, rice husk ash, and sugar cane bagasse ash, is increasing significantly in those countries that produce large amounts of these wastes that cause severe environmental issues if dumped in open fields (Binici et al., 2008; Martirena and Monzó, 2018). Previous studies show that sugar cane bagasse ash, which is a byproduct of the sugar cane industry, can be an effective material to be used in producing sustainable concrete (Ganesan et al., 2007; Aigbodion et al., 2010). Bagasse, a residue remaining after the extraction of juice from sugarcane is subsequently used in some industries as a primary source of energy (Frías et al., 2011). When it is burned as a fuel, it leaves bulk ash called bagasse ash (Loh et al., 2013). The burning of bagasse material at the temperature of 600–700°C produces amorphous silica, which eventually results in its substantial pozzolanic reactivity (Moretti et al., 2018). The estimated bulk production of bagasse after juice extraction of sugarcane is 600 Mt, which is between 40 and 50% of the total weight of annually produced sugarcane in the world (Shafiq et al., 2018). Among the largest sugarcane-producing countries, Pakistan is ranked fifth in the world, after Brazil, India, China, and Thailand, with an annual production of approximately 65.451 Mt. After burning the bagasse as a source of fuel, the ash waste is disposed of in landfills, which is causing serious environmental problems (Chusilp et al., 2009).

However, the utilization of this bagasse ash waste in concrete as a partial substitute for cement provides significant benefits in terms of reducing construction costs as well as greenhouse gas emissions. This is because bagasse ash contains high amounts of amorphous silica and aluminum oxides, which are necessary for a material to be pozzolanic (Ganesan et al., 2007; Frías et al., 2011; Bahurudeen et al., 2015).

Some researchers have reported that the pozzolanic reactivity of bagasse may improve the compressive strength of concrete and enhance other mechanical and durability-related properties (Rukzon and Chindaprasirt, 2012; Somna et al., 2012; Akkarapongtrakul et al., 2017). Since the main compound in bagasse ash is silica oxide, several searchers have reported its potential use in concrete. According to Malyadri and Supriya (2015), the strength parameters of concrete increased by using 5% sugarcane bagasse ash as a partial substitute for cement. A very similar trend of strength improvement was also reported in another study by Mangi et al. (2017). Whereas Kawade et al. (2013) concluded that up to 15% of sugarcane bagasse ash can be used favorably without compromising the primary properties of concrete. Shafiq et al. (2018) reported a considerable improvement in the compressive strength of concrete utilizing 20% sugarcane bagasse ash. Moreover, a significant improvement was also seen in the fresh, mechanical and durability properties of concrete. Ganesan et al. (2007) also reported an optimum substitution of 20% sugarcane bagasse ash for cement without compromising the desired properties of concrete. Although the utilization of ground bagasse ash (GBA) in concrete has been widely explored and well documented by many researchers, its efficiency in ECCs is still a novel topic to explore. Being a modern day construction material, ECC produced using GBA can be useful in repair works and prefabricated building components where high ductility is required.

Therefore, the primary objective of this study was to evaluate the performance of different proportions of GBA with PVA fibers on the mechanical properties of ECCs. For this purpose, the detailed investigations of the compressive strength, direct tensile strength, and flexural strength of ECCs were carried out. The idea of such a detailed investigation is due to the target of this research, which is to obtain the optimum content of GBA as a partial substitute for cement in ECCs with the maximum gain in terms of mechanical performance, as well as economic and environmental sustainability.

MATERIALS AND METHODS

Materials

Ordinary Portland Cement (OPC)

The cement used in this study was Type-I ordinary Portland cement (OPC) conforming to the requirements of ASTM C150-07 (2007). The specific surface area and density of the cement were 2670.3 cm^2/g and 3.15 g/cm^3, respectively. The X-ray fluorescence (XRF) analysis was performed to determine the chemical composition of the cement. **Table 1** shows the chemical composition of the cement used in this research.

TABLE 1 | Chemical composition of cement and bagasse ash.

Oxides composition	SiO_2	Fe_2O_3	Al_2O_3	CaO	Na_2O	MgO	SO_3	LOI	Physical properties	
									Blaine fineness (cm^2/g)	Density (g/cm^3)
						(%)				
Cement	18.4	3	5.6	66.8	0.13	1.4	1.3	2	2670.3	3.15
Bagasse ash	66.70	1.53	9.70	10.07	4.14	4.60	–	7.4	2850.8	2.25

Polyvinyl Alcohol (PVA) Fibers

Kuraray polyvinyl alcohol (PVA) fibers of diameter 14.3 μm were used in this research as a reinforcement for the ECC (**Figure 1**).

These fibers were very thin, similar to hairs, and flexible enough to prevent the generation of micro cracks. The density of the PVA fibers was 1.3 g/cm^3. **Table 2** shows the detailed physical properties of PVA fibers. The PVA characteristics data shown in **Table 2** were obtained from the manufacturer.

Bagasse Ash

Boiler-fired bagasse ash waste was collected from the sugar industry located in Sakhakot Malakand agency, Pakistan. To

FIGURE 1 | Polyvinyl alcohol fibers.

TABLE 2 | Physical properties of polyvinyl alcohol (PVA) fibers.

Manufacturer	Kurary
Origin	Japan
Color	White
Diameter (μm)	14.3
Length (mm)	8.0
Aspect ratio (l/d)	560
Tensile strength (MPa)	1716
Density (g/cm^3)	1.3
Elongation (%)	6.9

enhance the pozzolanic reactivity, the bagasse ash waste was treated using various processes, including burning, sieving, grinding, and chemical activation. These methods were efficiently utilized in combinations such that the bagasse ash waste attained the highest achievable pozzolanic reactivity. The bagasse ash collected from the sugar industry was further burned at 700°C for 90 min followed by cooling at room temperature. After cooling, the ash was stored in airtight containers until further testing. The burned bagasse ash stored in airtight containers was composed of both entirely burned (fine) and unburned (coarse fibrous) particles. The unburned coarse fibrous particles with high carbon content and without silica were not desired and, therefore, were completely separated by sieving through a 300-μm sieve to obtain only the fine particles for further processing. According to Bahurudeen et al. (2015), the burned bagasse ash passing the sieve 300-μm leaves only fine particles that are rich in silica content. **Figures 2A,B** show the appearance of the bagasse ash before and after sieving, respectively. The fine bagasse ash after grinding is shown in **Figure 2C**.

Grinding of the bagasse ash

Following heat treatment and sieving, the mechanical treatment of fine bagasse ash was carried out in a ball mill. The role of mechanical grinding in improving the performance of potential cement substitute materials is a well-established fact. In this study, the purpose of the mechanical grinding of bagasse ash was to increase its surface area and obtain its optimized value by varying the grinding times as 15, 30, 45, and 60 min. The speed of grinding was kept constant at 66 revolutions per minute and the grinding media-to-ash ratio was 5:1 by weight (i.e., 5 kg of balls to 1 kg of ash).

Mix Proportions

The constituents used in the production of ECC blends contained OPC, GBA, PVA fibers, and sand. Four different ECC mixes were designed by increasing the amount of GBA (0, 10, 20, and 30%) as a partial substitute by mass of cement. The water-to-binder ratio and the amount of PVA fibers were kept constant in all the ECC mixes at 0.40 and 1.5% of total mix volume, respectively. The detailed experimental matrix for the mix designs is summarized in **Table 3**. All the ECC mixes were labeled with a unique identity, i.e., CM for control mix without GBA, whereas the mixes containing 10, 20, and 30% GBA were identified as 10ECC, 20ECC, and 30ECC, respectively. The different proportions of bagasse ash in this study (10–30%) were selected based on the findings of

FIGURE 2 | Bagasse ash: **(A)** after heat treatment at 700°C for 90 min, **(B)** passed the 300-µm sieve after heat treatment, and **(C)** ground in a ball mill for 60 min after sieving.

TABLE 3 | ECC mix proportions for the control and mixes containing different percentages of GBA.

Mix ID	Mix quantities for 1 m³ ECC (kg)						
	W/B	Cement	Water	GBA	Sand	PVA fibers	Super plasticizers (% of binder)
CM	0.40	704	282	–	2112	26	1
10ECC	0.40	634	282	70	2112	26	1
20ECC	0.40	563	282	141	2112	26	1
30ECC	0.40	493	282	211	2112	26	1

previous studies (Ganesan et al., 2007; Bahurudeen et al., 2015; Joshaghani et al., 2016) as well as the trial tests. The main objective was to evaluate the synergy of different percentages of bagasse ash in ECC.

Mixing and Casting

The ingredients of the ECC mixes were added into the mixer in this order: sand, cement, PVA fibers, GBA. After adding the desired quantities to the mixer, the ingredients were thoroughly mixed for two minutes. Subsequently, the water and super plasticizers were added to the dry mixture and mixed for another 2 min. Eventually, the PVA fibers and GBA were slowly added into the mortar and mixed until all the fibers were uniformly dispersed. Immediately after mixing, the mixtures were cast into molds and stored under standard laboratory conditions of temperature and humidity. Three gang mortar steel molds (50 mm cube), coupon shaped steel molds (152 mm × 76 mm × 13 mm), and wooden prisms (320 mm × 40 mm × 12 mm) were used to cast mortar specimens for compressive strength tests, uniaxial tensile strength tests, and four-point bending tests, respectively. All the specimens were demolded after 24 h of casting and moist cured at 24 ± 2°C until the age of testing.

Test Methods

The pozzolanic activity of bagasse ash was determined using the Chapelle test. The XRF, X-ray diffraction (XRD) pattern, and fineness were also determined. The microstructure of the GBA particles was analyzed through the scanning electron microscopy (SEM) technique. Together with direct tensile strength and flexural strength tests, the flexural behavior of ECCs containing different proportions of BA was also investigated.

Fineness and Pozzolanic Reactivity of the Bagasse Ash

The fineness values of the cement and GBA were determined by using the Blaine air permeability apparatus in accordance with ASTM C204 - 11 (2011). The influence of the grinding time on the total surface area of the GBA is shown in **Figure 3**. It can be seen that the surface area of the bagasse ash before grinding was 2067.8 cm²/g, which, compared to that of cement (2670.3 cm²/g), is lower. However, the surface area of the bagasse ash increased after grinding and gradually continued increasing with increased grinding. The desired surface area (greater than that of cement) was attained, corresponding to grinding for 60 min. Bahurudeen and Santhanam (2015) concluded that the pozzolanic reactivity of
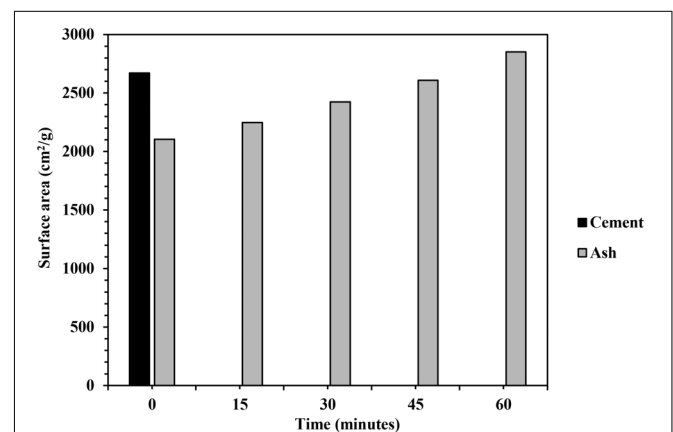

FIGURE 3 | Influence of grinding duration on the surface area of bagasse ash and its comparison with cement.

GBA is enhanced significantly when its surface area is equivalent to that of cement.

Following the grinding phase, the pozzolanic reactivity of the bagasse ash obtained from grinding for 60 min was determined by the Chappelle test in accordance with French norm, NF P 18-513 (Association Française de Normalisation [AFNOR], 2012; Pontes et al., 2013). The Chappelle test was performed to determine the reduction in $Ca(OH)_2$ due to its reaction with siliceous or alumina-silicates present in pozzolans in GBA. The Chappelle activity test chemically determines the amount of lime utilized by a pozzolan. The amount of lime utilized is directly proportional to the pozzolanic activity of the material. The results of the current Chapelle test on the GBA satisfied the minimum requirements set for pozzolanic activity (330 mg of CaO/g of pozzolan) due to its highly active amorphous silica (Li et al., 2004). This finding clearly suggested that the GBA is chemically reactive in nature and therefore suitable for its use as a sustainable cement substitute material.

Scanning Electron Microscopy (SEM) of the Bagasse Ash

The morphological investigation of some selected samples of GBA was conducted using SEM (JSM5910 JEOL, Japan). **Figure 4** shows the micrographs of studied samples at magnification ranges from X500 to X2000.
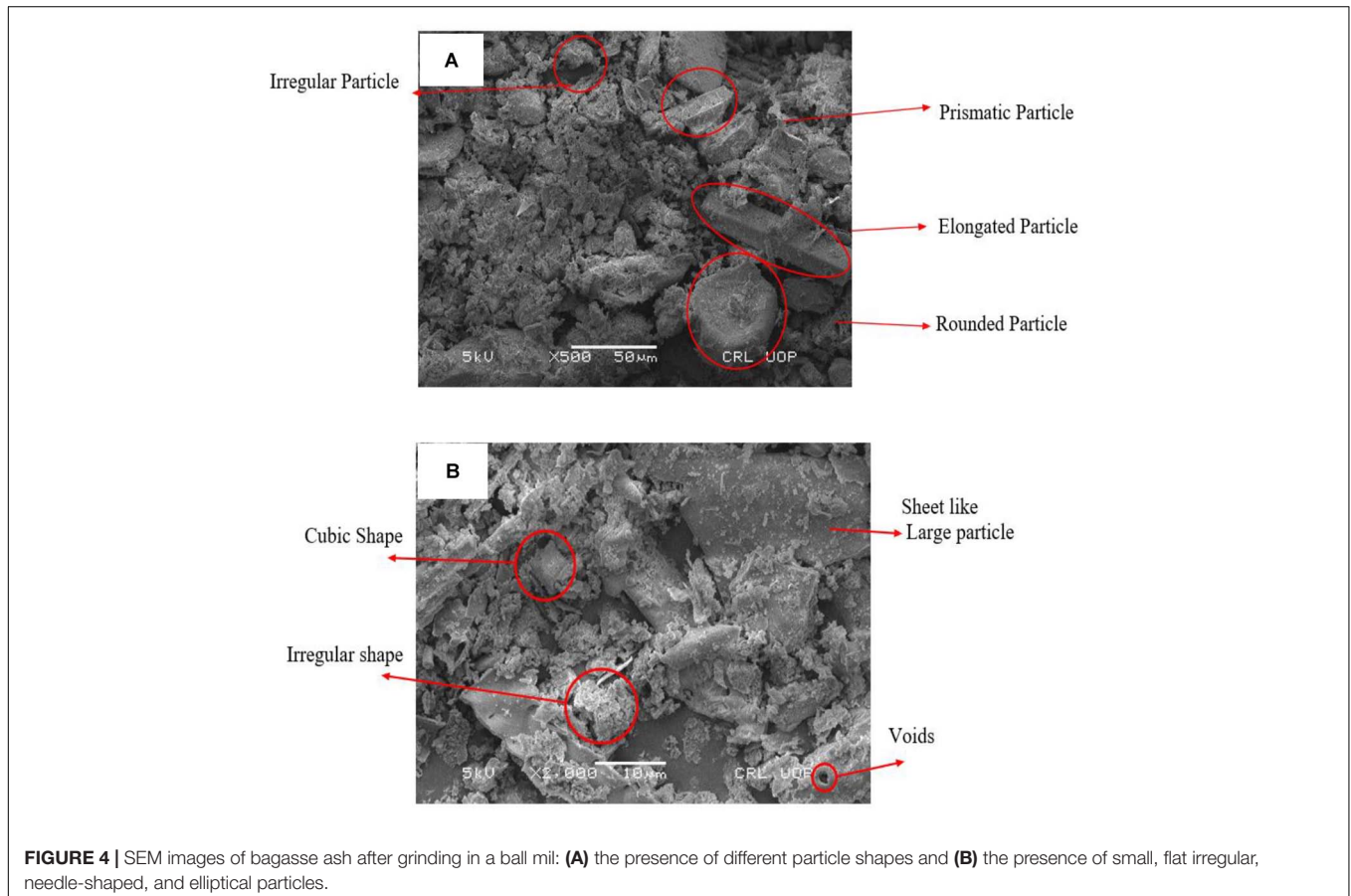
From these micrographs, it can be seen that the ash sample contains many different particle shapes, such as rounded, elongated, irregular, and prismatic (**Figure 4A**). The sizes of particles range from 10 to 50 μm. Moreover, **Figure 4B** shows small, flat irregular, needle-shaped, and elliptical particles.

Compressive Strength

This test was performed to investigate the compressive strength evolution of all the ECC mixes. A total of nine 50 mm cube specimens were cast for each mix (CM, 10ECC, 20ECC, and 30ECC) to test three identical specimens at ages of 14, 28, and 91 days. The tests were performed in accordance with ASTM C109 / C109M - 16a (2016) using a compression machine as shown in **Figure 5A**. According to ASTM C109, the loading rate in the compression machine was kept at 0.91 kN/s for all specimens.

Direct Tensile Test

Just like compression tests, nine coupon specimens having dimensions of 152 mm × 76 mm × 13 mm were cast for each mix to carry out uniaxial tensile tests at ages of 14, 28, and 91 days. A series of direct tensile tests were performed using a universal testing machine (**Figure 5B**). The purpose of these tests is to investigate the influence of the different amounts of GBA on tensile strength and to study the tensile stress-strain and strain-hardening behavior of the ECC mixes at desired
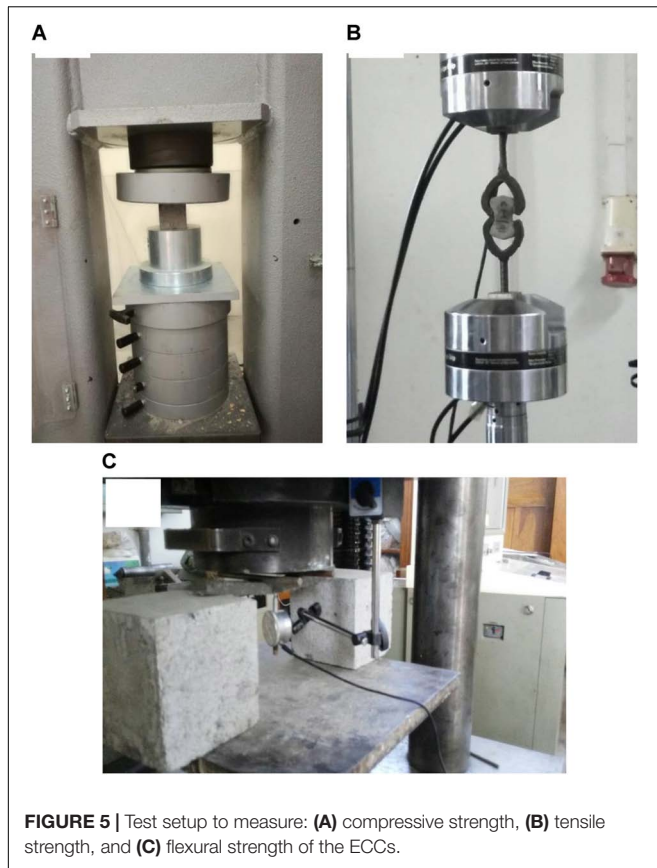

FIGURE 4 | SEM images of bagasse ash after grinding in a ball mil: **(A)** the presence of different particle shapes and **(B)** the presence of small, flat irregular, needle-shaped, and elliptical particles.

FIGURE 5 | Test setup to measure: (A) compressive strength, (B) tensile strength, and (C) flexural strength of the ECCs.

FIGURE 6 | Comparison of compressive strength with aging among CM and ECC mixes containing different percentages of GBA.

RESULTS AND DISCUSSION

Compressive Strength

Figure 6 shows the comparison of the strength results of all four ECC mixes according to different proportions of GBA and curing ages (14, 28, and 91 days). At early ages (14 days of curing), all the ECC mixes containing GBA possessed lower compressive strength compared to that of the control mix. Moreover, the reduction in compressive strength gradually increased with increasing amounts of GBA in the mix. This phenomenon of strength reduction can be attributed to slight or no pozzolanic activity at earlier stages. However, with increasing curing age, this phenomenon of strength reduction with increasing amounts of GBA was completely reversed, particularly at later ages such as 91 days of curing. A similar behavior of decreasing strength at early ages and then increasing strength with curing ages was also reported in the literature (Arenas-Piedrahita et al., 2016; Joshaghani et al., 2016). The mineralogy (**Table 1**) as well as the pozzolanic reactivity results obtained by the Chappelle test reflected predominate behavior of GBA in gaining later age strengths. Moreover, the particle characteristics of calcined GBA observed by SEM (**Figure 4**) also suggests a denser and improved micro-structural phase of mortars containing different percentages of GBA as compared to CM. The size and the shape of particles affect both the fresh as well as the hardened properties of cement matrix in a significant manner.

At 28 days, only the ECC containing 10% GBA (10ECC) produced better compressive strength compared to that of the control mix, while the other two mixes (20ECC and 30ECC) still possessed lower values. The inclusion of 10% GBA in the ECC mix demonstrated 3 and 7% higher strength than that of the CM at 28 and 91 days, respectively. The gain in strength could be due to the consumption of free lime available in the matrix. The mix containing 20% GBA (20ECC) exhibited an approximately 6% reduction in compressive strength at 28 days of curing, while the compressive strength increased by 3% at an age of 91 days.

testing ages. The specimens were loaded to a constant cross-head speed of 0.003 mm/s. To measure strain, electrical resistance strain gauges (Tokyo Sokki PFL-20-11-3L) were mounted on to the surface of coupon specimens and the strain data were recorded using a data logger. Along with strain measurements, the elongation of the coupon specimen with loading was also measured using a displacement transducer, simultaneously using the same data logger.

Four-Point Bending Test

The flexural strengths of the ECC mixes were measured by using the four-point loading method as specified by ASTM C348 - 14 (2014). For this purpose, nine rectangular beams of size 320 mm length × 40 mm height × 12 mm thickness were cast for each mix to test three identical specimens at ages of 14, 28, and 91 days. As shown in **Figure 5C**, the clear span (the span between the supports) was divided into three equal parts to have two points to transmit the load. A deflection gauge was attached to the middle bottom surface of the beams to monitor deflection at regular intervals of loading. Eventually, from this test, the values of the first crack load and flexural strength were measured. Moreover, the load-deflection curves were drawn using the measured values of load and deflection to compare the toughness and deflection behavior of different mixes.
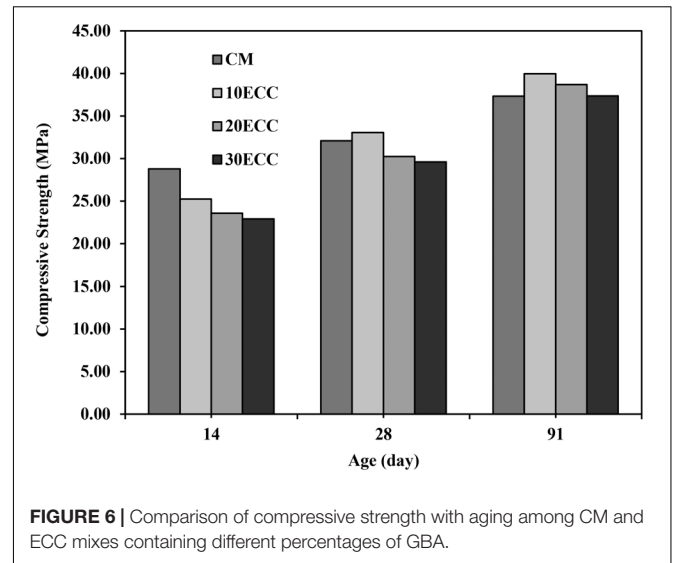
Similar to 20ECC, the reduction in strength continued for 30ECC at 28 days and ended up at almost the same strength as that of CM at 91 days. The reason for the strength reduction in 20ECC and 30ECC at 28 days can be associated with decreased cement content and therefore slow pozzolanic reactivity (Bahurudeen et al., 2015). Overall, the current results indicated safe use of GBA in lower amounts, such as up to 10%, in producing optimized ECCs without compromising the required compressive strength.

Tensile Strength and Load-Strain Behavior of the ECCs

Figure 7 shows the comparison of the tensile strength results among different ECC mixes with and without GBA according to different curing ages (14, 28, and 91 days). As expected, the trend of tensile strength development among all ECC mixes followed almost the same pattern as that of the compressive strength at all ages except at 91 days. For instance, similar to the compressive strength at an early age (14 days), the tensile strength also remained lower than that of the CM in all the ECC mixes and decreased gradually with the increasing percentage of GBA. Moreover, at 28 days, only 10ECC possessed higher tensile strength than that of CM, while the other ECC mixes exhibited lower tensile strength. Contrary to the compressive strength results, the tensile strengths of the ECC mixes remained lower at 91 days than that of CM, except 10ECC, which exhibited higher tensile strength. Overall, the results indicated that the ECC containing 10% GBA (10ECC) produced the best results among all the mixes in terms of tensile strength. The tensile strengths were approximately 8.33 and 7.40% higher than those of the CM at 28 and 91 days, respectively. Based on the tensile strength comparison among the different ECC mixes, the use of 10% GBA can be recommended in producing optimized ECCs without compromising tensile strength.

Figure 8 shows the load vs. strain relationship among the different ECC mixes according to curing ages (14, 28, and
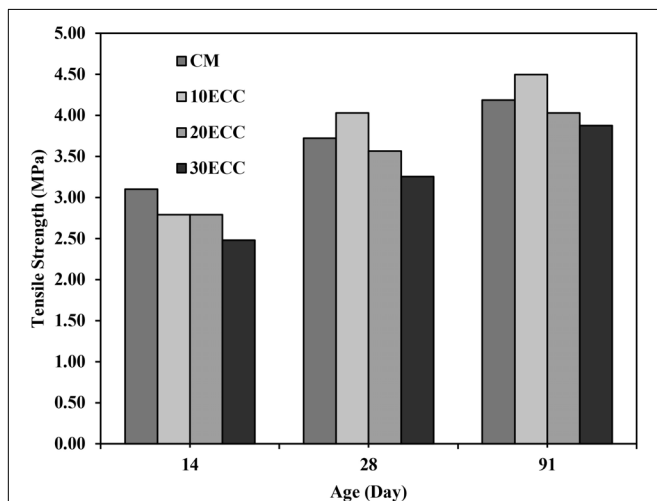
FIGURE 7 | Comparison of tensile strength with aging among CM and ECC mixes containing different percentages of GBA.
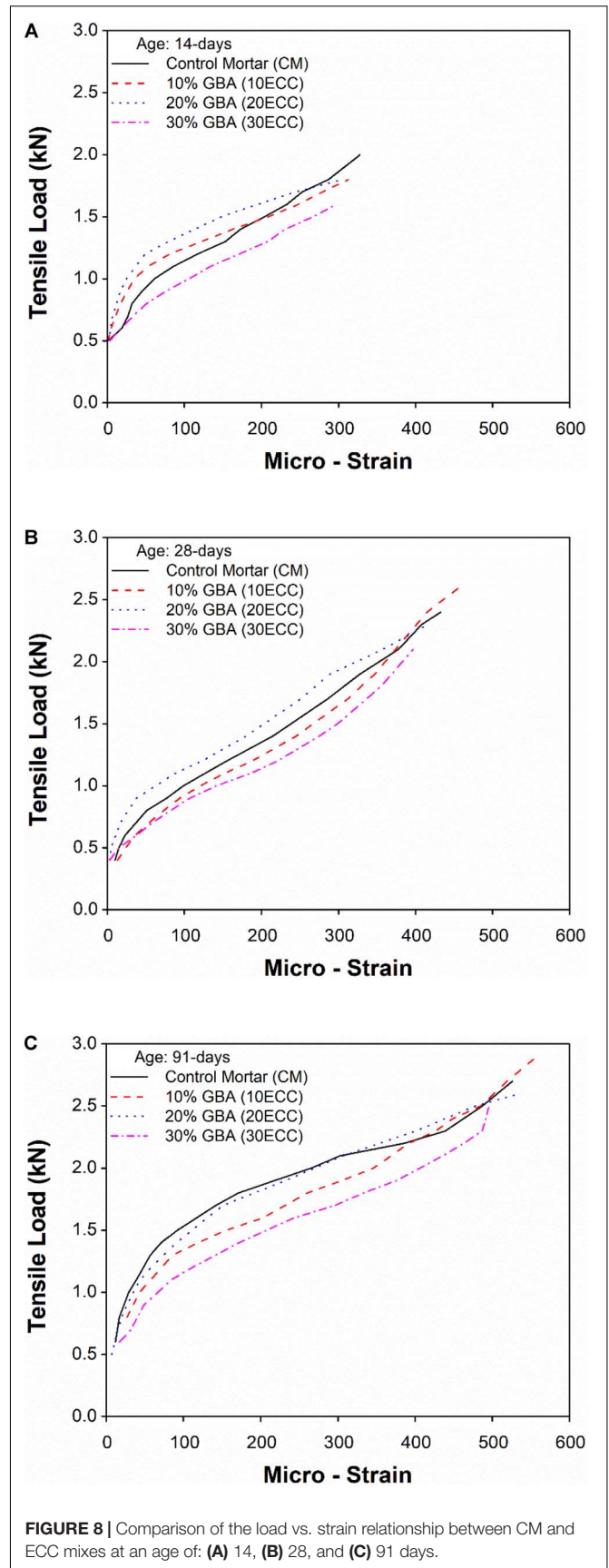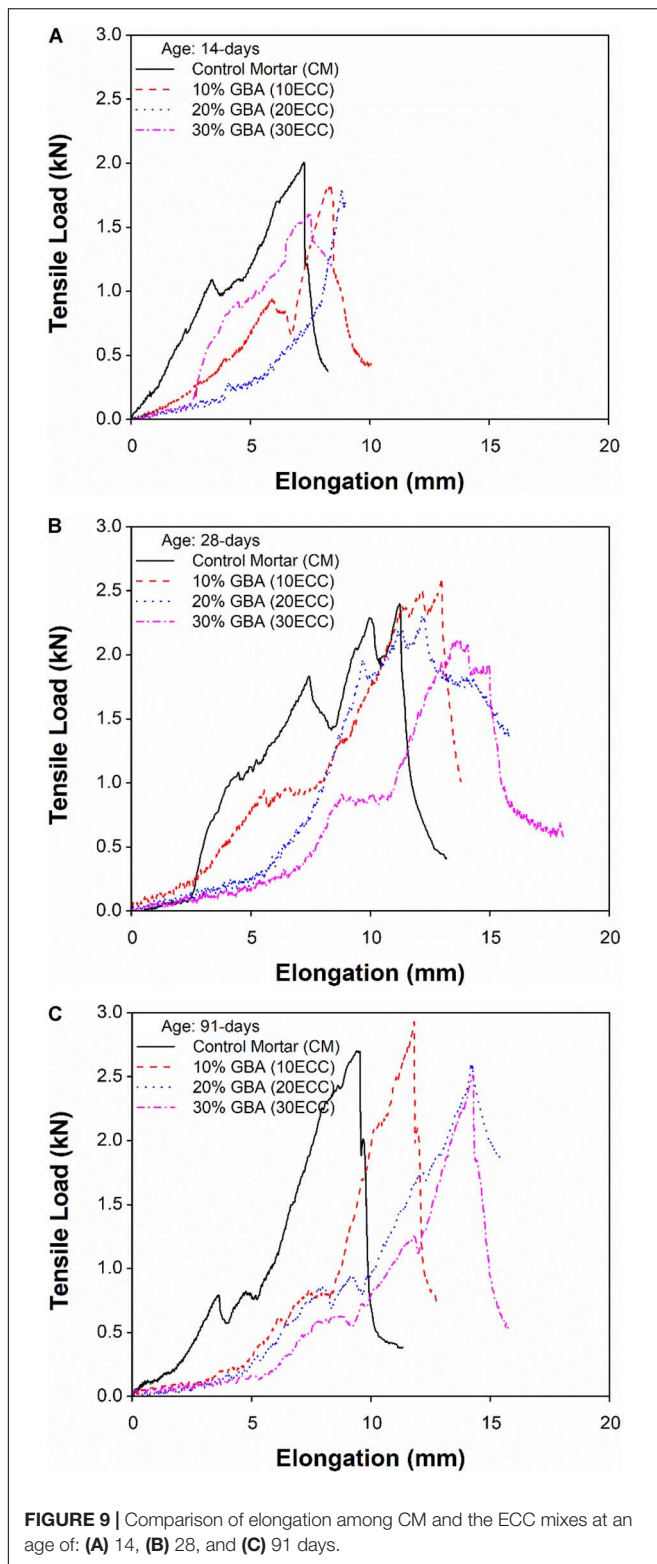
FIGURE 8 | Comparison of the load vs. strain relationship between CM and ECC mixes at an age of: **(A)** 14, **(B)** 28, and **(C)** 91 days.

FIGURE 9 | Comparison of elongation among CM and the ECC mixes at an age of: **(A)** 14, **(B)** 28, and **(C)** 91 days.

91 days). It may be worth noting that the strain data used in **Figure 8** were directly obtained from electrical resistance strain gauges (Tokyo Sokki PFL-20-11-3L) mounted on the surfaces of the coupon specimens. At an age of 14 days, a slightly better

response to loading was observed in both 10ECC and 20ECC compared to that of CM. It was further noted that 20ECC performed better than CM at all load levels regardless of curing ages. However, 10ECC showed more strain compared to that of CM at all load levels at both 28 and 91 days, except toward failure where it exhibited lower strain at higher loads than that of CM.

Eventually, the current load-strain relation demonstrated a toughness behavior for all the ECC mixes (10ECC and 20ECC GBA) comparable to that of CM. The values of toughness were not calculated due to damage to the strain gauges corresponding to the failure loads. The highest value of strain corresponding to the failure load of 2.9 kN was observed in 10ECC as 558 μ at 91 days. At 28 days, 10ECC exhibited the highest strain among all the mixes, which was equal to 457 μ, corresponding to a failure load of 2.6 kN. This increase in the microstrain in 10ECC is 5.54% and 6.08% more than the corresponding values of CM at 28 and 91 days, respectively.

Elongation With Load

In addition to the measurement of microstrain with respect to load as discussed in the previous section, the elongation with respect to loading for CM as well as all the ECC mixes (10ECC, 20ECC, 30ECC) was also measured using displacement transducers. **Figure 9** shows the comparison of the load-elongation behavior among CM and the ECC mixes with aging. In addition, the detailed results of current investigations on the tensile strength-related properties of ECC mixes (first crack load, maximum load, and elongation) are also listed in **Table 4**.

Compared to CM, a slight increase in elongation was observed in all the ECC mixes (10ECC, 20ECC, and 30ECC) irrespective of aging (14, 28, or 91 days). Moreover, the elongation increased with increasing percentages of GBA, particularly at later ages (28 and 91 days). Such elongation behavior clearly indicated improved ductility of the ECC mixes containing different percentages of GBA. At early ages (14 days), although the elongation increased in all the ECC mixes compared to that of CM, it decreased with increasing percentages of GBA from 10 to 20% and 20 to 30%. It is expected that the decrease in elongation at early ages with increasing percentages of GBA might be due to the gradually decreasing amount of cement and eventually the occurrence of early failure at relatively smaller loads compared to that of 10ECC. Elongation significantly increased in all mixes with aging from 14 to 28 days, which must be due to the increased hydration reaction with aging. More importantly, the intensity of elongation with aging increased with increasing amounts of GBA. For instance, the increase in elongation with aging from 14 to 28 days was calculated as 37, 76, and 116% in 10ECC, 20ECC, and 30ECC, respectively. This clearly indicated an improved mechanical behavior of the ECC mixes with increasing amounts of GBA. However, unlike early ages, a slight decrease in elongation was observed in all the mixes with aging from 28 to 91 days. This must be due to the small increase in brittleness, as the strengths of the mixes increased at 91 days. A decrease in elongation by 7.43, 2.5, and 13% was calculated from 28 to 91 days for 10ECC, 20ECC, and 30ECC, respectively. The smallest reduction in elongation in 20ECC at 91 days indicated that the 20% GBA-blended ECC mix

Mix ID	First crack load (kN)			Maximum load (kN)			Maximum elongation (mm)		
				Age (days)					
	14	28	91	14	28	91	14	28	91
CM	0.854	0.875	0.822	2.010	2.402	2.703	8.236	13.194	11.353
10ECC	0.897	0.937	0.691	1.810	2.601	2.931	10.051	13.816	12.789
20ECC	0.878	0.967	0.763	1.802	2.311	2.599	8.994	15.813	15.418
30ECC	0.789	0.943	0.659	1.605	2.121	2.510	8.410	18.146	15.793

exhibited the best mechanical behavior in terms of its ductility among all the mixes.

All the tested ECC samples showed a continual increase in load-carrying capacity after the appearance of the first crack. It can be seen from the maximum load values listed in **Table 4** that the load-carrying capacity increased continuously with aging regardless of the mortar type (control or other mortars containing any percentage of GBA) and decreased with increasing amounts of GBA. The decrease in the maximum load-carrying capacity is obviously due to decreased amounts of binder with increasing amounts of GBA (10–20, then 30%).

Unlike the trend of the maximum loads, the load corresponding to the first crack increased in mortars containing GBA, particularly at ages of 14 and 28 days. The first crack loads continued increasing with aging (14–28 days) as well as with increasing amounts of GBA. However, at 14 days, the trend of the increasing first crack load was rather insignificant and even a decrease was observed in the mortar containing 30% GBA (30ECC). This must be due to the reduced hydration reaction because of a smaller amount of cement in 30ECC, thus leading to low stiffness of the mortar matrix and early cracking. At later ages (91 days), the first crack load compared to that of early ages decreased in all mortars with and without GBA. The reason is that the degree of brittleness of the cementitious composites increased with aging. However, the lowest reduction in the first crack load compared to that of CM was recorded in 20ECC. The reduction in the first crack loads in 10ECC, 20ECC, and 30ECC at the age of 91 days was recorded as 16, 7, and 20% of that of CM, respectively.
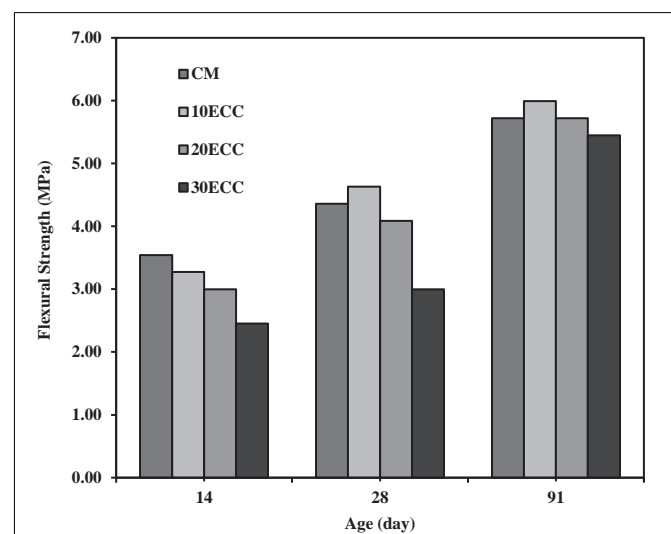
Flexural Strength

Figure 10 shows the influence of different proportions of GBA on the flexural strength of ECC mixes with aging. The flexural strength closely followed a trend similar to that of the compressive strength where the flexural strength of the ECCs containing GBA remained lower than that of the CM at early ages (14 days). The trend of gradual reduction with increasing percentages of GBA at early ages demonstrated decreased pozzolanic activity with increasing GBA. This trend of decreasing flexural strength in the ECCs with increasing percentages of GBA continued at 28 days as well, except in 10ECC. Like compressive strength, the flexural strength of 10ECC exceeded that of CM at both 28 and 91 days by 6.6 and 4%, respectively. Moreover, the reduction in the flexural strengths in 20ECC and 30ECC

compared to that of CM reduced significantly at 91 days and even turned almost identical to that of CM in 20ECC. This is attributed to increased pozzolanic reactivity with increasing amounts of GBA with aging.

Load Deflection Curves

To investigate the influence of GBA on ductility, the mid-span deflection of beams was measured with aging. The experimental set up of flexural tests on rectangular beams with a deflection gauge attached to the middle bottom of the specimens is shown in **Figure 5**. The load on the beams gradually increased until its failure, and the deflection corresponding to the load was automatically logged using a data logger. **Figure 11** shows a comparison of the load-deflection relationship among the CM and different ECC mixes with respect to different curing ages. As mentioned earlier in Section "Materials and Methods," nine identical specimens were cast for each mix to test three specimens at each age (14, 28, and 91 days). The presented curves in **Figure 11** are an average of three samples. It was noted that the maximum deflection corresponding to the failure load ranged between 3 and 6 mm depending on the type of ECC (10ECC, 20ECC, or 30ECC) and aging (14, 28, or 91 days).

FIGURE 10 | Comparison of flexural strength with aging among CM and the ECC mixes containing different percentages of GBA.

FIGURE 11 | Comparison of the load-deflection behavior among the CM and ECC mixes at an age of: **(A)** 14, **(B)** 28, and **(C)** 91 days.
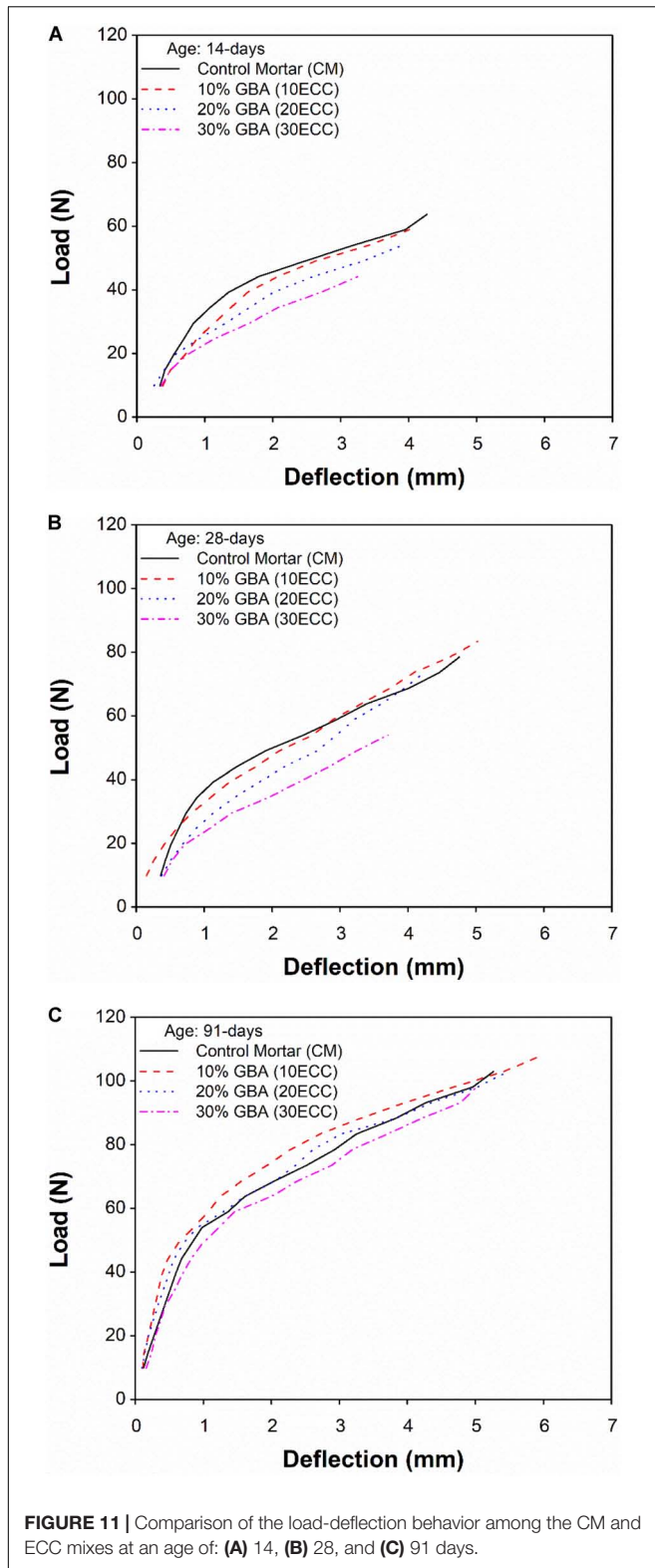
At early ages such as 14 days, the maximum deflection among all the ECC mixes occurred in CM, while at the same age, both the failure load as well as its corresponding deflection decreased

gradually with increasing amounts of GBA in all the studied mixes. At any particular load level, deflection in the ECC mixes increased with increasing amounts of GBA. However, the load-deflection behavior of 10ECC was almost identical to that of CM. Moreover, the load-deflection behavior of ECCs containing GBA significantly improved with aging from 14 to 28 days and from 28 to 91 days. From **Figures 11B,C**, it can be seen that the resistance to deflection as well as the load-carrying capacity of 10ECC is greater than those of CM at both 28 and at 91 days. Similar to 10ECC, specimen 20ECC exhibited identical or slightly better load-deflection responses than that of CM at later ages. Considering the above discussion, the use of 10% GBA is recommended in producing sustainable ECCs as it exhibited the highest ductility among all the ECC mixes used in this study.

CONCLUSION

This research was carried out to study the potential use of GBA as a partial substitute for cement to produce an economical and sustainable ECC. For this purpose, three different percentages of GBA were selected (10ECC, 20ECC, and 30ECC) to evaluate the improvement in their mechanical performance factors, such as strength, deflection, ductility, first crack load, maximum loads, and elongation behavior. Considering the current findings, the following are the main conclusions drawn from this experimental study.

1. The results indicated that the compressive strength of ECC mixes gradually decreased with increasing amounts of GBA. The addition of GBA in ECCs reduced the compressive strength at early ages (14 days), which, however, was enhanced significantly at later ages. The mix containing 10% GBA (10ECC) exhibited the highest compressive strength among all the other ECC mixes, including CM, at the age of both 28 and 91 days. The compressive strength of 10ECC in comparison to that of CM was found to be higher, almost 3 and 7% higher at 28 and 91 days, respectively. The other ECC mixes with high amounts of GBA (20ECC and 30ECC) produced slightly higher strengths than that of CM only at 91 days.

2. Direct tensile and flexural strength trends similar to that of compressive strength were observed for all the mixes except that both 20ECC and 30ECC possessed slightly smaller tensile strengths than that of CM at 91 days. However, the flexural strengths for 20ECC and 30ECC are almost identical and only slightly smaller than that of CM at 91 days. Moreover, it was observed that the influence of increasing the amount of GBA on the reduction in tensile and flexural strengths decreased with aging from 14 to 28 and then from 28 to 91 days. Like with compressive strength, 10ECC demonstrated higher direct tensile and flexural strengths than those of CM. The results indicated 8.33 and 7.4% higher tensile strengths, and 6.6 and 4% higher flexural strengths than those of CM at 28 and 91 days, respectively.

3 A comparable tensile load-to-strain relation among the ECC mixes containing 10 and 20% GBA (10ECC and 20ECC) and CM was observed irrespective of aging. At later ages (28 and 91 days), in particular, 10ECC exhibited the highest failure load with the highest corresponding tensile strain. Consequently, it may be worth noting that the ECC mixes (10ECC and 20ECC) demonstrated acceptable ductility and toughness behavior for their potential sustainable engineering applications.

4 The direct tensile tests showed a continuous increase in load-carrying capacity after the appearance of a first crack in all the mixes. Moreover, it was noticed that the elongation in all the GBA-blended ECC mixes increased significantly with increasing amounts of GBA and with aging, particularly, at later curing ages.

5 The load-deflection results indicated that the failure load as well as its corresponding deflection decreased gradually with increasing amounts of GBA. At any particular load level, deflection in the ECC samples increased with increasing amounts of GBA. However, the load-deflection behavior of 10ECC is almost identical to that of CM. Moreover, the load-deflection behavior of the ECCs containing GBA significantly improved with aging, for instance, from 14 to 28 days and from 28 to 91 days. In comparison to those of CM, the ECC with 10% GBA demonstrated greater resistance to deflection as well as higher load-carrying capacity at both 28 and at 91 days. Moreover, the ECC containing 20% GBA also exhibited identical or slightly better load-deflection responses than that of CM at later ages.

6 Considering the above discussion and the most important findings of this study, 10% GBA can be considered as the optimum replacement of cement in producing a sustainable ECC as it exhibited improved strengths (compressive, tensile, and flexural), better resistance to deflection, and improved ductility compared to those of all the ECC mixes used in this study.

DATA AVAILABILITY STATEMENT

The datasets generated for this study are available on request to the corresponding author.

AUTHOR CONTRIBUTIONS

MNA, MA, RK, and KK contributed to the design of this research and critically analyzed and discussed the results of this research. DS, SA, and SK contributed to the methodology and performance of the experiments, including collecting bagasse ash (BA) and other ingredients, burning BA, sieving and grinding BA, and mixing, casting, demolding, and curing the specimens, performing XRD analysis and mechanical testing, and preparing the initial draft. MNA, MA, and RK reviewed, edited, and prepared the final draft of this manuscript.

FUNDING

ACKNOWLEDGMENTS

REFERENCES

Aigbodion, V. S., Hassan, S. B., Ause, T., and Nyior, G. B. (2010). Potential Utilization of Solid Waste (Bagasse Ash). *J. Min. Mater. Character. Eng.* 9, 67–77. doi: 10.4236/jmmce.2010.91006

Akkarapongtrakul, A., Julphunthong, P., and Nochaiya, T. (2017). Setting time and microstructure of Portland cement-bottom ash–sugarcane bagasse ash pastes. *Monatshef. Chem.* 148, 1355–1362. doi: 10.1007/s00706-017-1953-5

Al Qadi, A. N. S., and Al-Zaidyeen, S. M. (2014). Effect of fibre content and specimen shape on residual strength of polypropylene fibre self-compacting concrete exposed to elevated temperatures. *J. King Saud Univ. Eng. Sci.* 26, 33–39. doi: 10.1016/j.jksues.2012.12.002

Arenas-Piedrahita, J. C., Montes-García, P., Mendoza-Rangel, J. M., López Calvo, H. Z., Valdez-Tamez, P. L., and Martínez-Reyes, J. (2016). Mechanical and durability properties of mortars prepared with untreated sugarcane bagasse ash and untreated fly ash. *Constr. Build. Mater.* 105, 69–81. doi: 10.1016/j.conbuildmat.2015.12.047

Association Française de Normalisation [AFNOR] (2012). Standard NF P 18-513/2012-Pozzolanic Addition for Concrete-Metakaolin-Definitions, Specifications and Conformity Criteria; La Plaine Saint-Denis: AFNOR, 2012. Available at: https://www.boutique.afnor.org/standard/nf-p18-513/ addition-for-concrete-metakaolin-specifications-and-conformity-criteria/ article/760894/fa175740 (accessed April 23, 2018).

ASTM C109 / C109M - 16a (2016). *Standard Test Method for Compressive Strength of Hydraulic Cement Mortars (Using 2-in. or [50-mm] Cube Specimens).* Available at: www.astm.org (accessed April 23, 2018).

ASTM C150-07 (2007). *Standard Specification for Portland Cement; American Society for Testing and Materials.* Available at: www.astm.org (accessed April 23, 2018).

ASTM C204 - 11 (2011). *Standard Test Methods for Fineness of Hydraulic Cement by Air-Permeability Apparatus.* Available at: www.astm.org (accessed April 23, 2018).

ASTM C348 - 14 (2014). *Standard Test Method for Flexural Strength of Hydraulic-Cement Mortars; American Society for Testing and Materials.* Available at: www.astm.org (accessed April 23, 2018).

Bahurudeen, A., Kanraj, D., Gokul Dev, V., and Santhanam, M. (2015). Performance evaluation of sugarcane bagasse ash blended cement in concrete. *Cem. Concr. Compos.* 59, 77–88. doi: 10.1016/j.cemconcomp.2015.03.004

Bahurudeen, A., and Santhanam, M. (2015). Influence of different processing methods on the pozzolanic performance of sugarcane bagasse ash. *Cem. Concr. Compos.* 56, 32–45. doi: 10.1016/j.cemconcomp.2014.11.002

Binici, H., Yucegok, F., Aksogan, O., and Kaplan, H. (2008). Effect of corncob, wheat straw, and plane leaf ashes as mineral admixtures on concrete durability. *J. Mater. Civil Eng.* 20, 478–483. doi: 10.1061/(asce)0899-1561(2008)20:7 (478)

Chusilp, N., Jaturapitakkul, C., and Kiattikomol, K. (2009). Utilization of bagasse ash as a pozzolanic material in concrete. *Constr. Build. Mater.* 23, 3352–3358. doi: 10.1016/j.conbuildmat.2009.06.030

Frías, M., Villar, E., and Savastano, H. (2011). Brazilian sugar cane bagasse ashes from the cogeneration industry as active pozzolans for cement manufacture. *Cem. Concr. Compos.* 33, 490–496. doi: 10.1016/j.cemconcomp.2011.02.003

Ganesan, K., Rajagopal, K., and Thangavel, K. (2007). Evaluation of bagasse ash as supplementary cementitious material. *Cem. Concr. Compos.* 29, 515–524. doi: 10.1016/j.cemconcomp.2007.03.001

Joshaghani, A., Ramizanianpour, A. A., and Rostami, H. (2016). "Effect of incorporating sugarcane bagasse ash (SCBA) in mortar to examine durability of sulfate attack," in *Proceedings of the Second International Conference on Concrete Sustainability*, Madrid.

Kawade, U. R., Rathi, V. R., and Vaishali, D. G. (2013). Effect of use of bagasse ash on strength of concrete. *Intern. J. Innovat. Res. Sci. Eng. Technol.* 2, 2997–3000.

Klee, H. (2009). *The Cement Sustainability Initiative: Recycling Concrete-Summary*. Geneva: World Business Council for Sustainable Development (WBCSD).

Kumar, R., Mohd Yaseen, A. Y. B., Shafiq, N., and Jalal, A. (2017). Influence of metakaolin, fly ash and nano silica on mechanical and durability properties of concrete. *Key Eng. Mat.* 744, 8–14. doi: 10.4028/www.scientific.net/kem. 744.8

Li, V. C. (1993). From micromechanics to structural engineering – the design of cementitious composites for civil engineering application. *J. Struct. Eng. Earthquake Eng.* 10, 37–48.

Li, V. C. (2002). "Reflections on the research and development of engineered cementitious composites (ECC)," in *Proceedings of the JCI international Workshop – DFRCC*, Takayama.

Li, V. C. (2012). Tailoring ECC for special attributes: a review. *Int. J. Concr. Struct.* 6, 135–144. doi: 10.1007/s40069-012-0018-8

Li, V. C., Lepech, M., and Wang, S. (2004). "Development of green engineered cementitious composites for sustainable infrastructure systems," in *Proceedings of the Workshop on Sustainable Development and Concrete Technology*, ed. K. Wang (Beijing: Iowa State University), 181–191.

Li, V. C., Wu, C., Wang, S., Ogawa, A., and Saito, T. (2002). Interface tailoring for strain-hardening polyvinyl alcohol-engineered cementitious composites (PVA-ECC). *ACI Mater J.* 99, 463–472.

Liu, J. C., and Tan, K. H. (2018). Fire resistance of ultra-high performance strain hardening cementitious composite: Residual mechanical properties and spalling resistance. *Cem. Concr. Compos.* 89, 62–75. doi: 10.1016/j. cemconcomp.2018.02.014

Loh, Y. R., Sujan, D., Rahman, M. E., and Das, C. A. (2013). Review sugarcane bagasse - the future composite material: a literature review. *Resour. Conserv. Recy.* 75, 14–22. doi: 10.1016/j.resconrec.2013.03.002

Malyadri, T., and Supriya, J. (2015). Experimental study on bagasse ash in concrete by partially replacement with cement. *Int. J. of Comput. Eng. Res. Tre.* 2, 995–1001.

Mangi, S. A., Jamaluddin, N., Wan Ibrahim, M. H., Abdullah, A. H., Abdul Awal, A. S. M., and Sohu, S. (2017). Utilization of sugarcane bagasse ash in concrete as partial replacement of cement. *Mater. Sci. Eng. Conf. Ser.* 271:12001.

Martirena, F., and Monzó, J. (2018). Vegetable ashes as supplementary cementitious materials. *Cem. Concr. Res.* 114, 57–64. doi: 10.1016/j.cemconres. 2017.08.015

Moretti, J. P., Nunes, S., and Sales, A. (2018). Self-compacting concrete incorporating sugarcane bagasse ash. *Constr. Build. Mater.* 172, 635–649. doi: 10.1016/j.conbuildmat.2018.03.277

Pontes, J., Santos Silva, A., and Faria, P. (2013). Evaluation of pozzolanic reactivity of artificial pozzolans. *Mater. Sci. Forum* 730, 433–438. doi: 10.4028/www. scientific.net/msf.730-732.433

Rukzon, S., and Chindaprasirt, P. (2012). Utilization of bagasse ash in high-strength concrete. *Mater. Design.* 34, 45–50. doi: 10.1016/j.matdes.2011.07. 045

Shafiq, N., Hussein, A. A. E., Nuruddin, M. F., and Al Mattarneh, H. (2018). Effects of sugarcane bagasse ash on the properties of concrete. *P. I. Civil Eng. Eng. Su.* 171, 123–132.

Shi, L., Lin, S. T. K., Lu, Y., Ye, L., and Zhang, Y. X. (2018). Artificial neural network based mechanical and electrical property prediction of engineered cementitious composites. *Constr. Build. Mater.* 174, 667–674. doi: 10.1016/j.conbuildmat. 2018.04.127

Somna, R., Jaturapitakkul, C., Rattanachu, P., and Chalee, W. (2012). Effect of ground bagasse ash on mechanical and durability properties of recycled aggregate concrete. *Mater. Design.* 36, 597–603. doi: 10.1016/j.matdes.2011.11. 065

Wu, M., Johannesson, B., and Geikera, M. (2012). A review: Self-healing in cementitious materials and engineered cementitious composite as a self-healing material. *Constr. Build. Mater.* 28, 571–583. doi: 10.1016/j.conbuildmat.2011. 08.086

Zeman, F. (2009). Oxygen combustion in cement production. *Energy Proc.* 1, 187–194. doi: 10.1016/j.egypro.2009.01.027